ELSEVIER

International Journal of Mass Spectrometry 214 (2002) 257–267

International Journal of Mass Spectrometry

www.elsevier.com/locate/ijms

The role of oxygen in the formation of TNT product ions in ion mobility spectrometry

Keith A. Daum, David A. Atkinson, Robert G. Ewing*

Department of Chemistry, Idaho National Engineering and Environmental Laboratory, Idaho Falls, ID 83415-2208, USA

Received 20 February 2001; accepted 6 December 2001

Abstract

The atmospheric pressure ionization of 2,4,6-trinitrotoluene (TNT) in air yields the $(TNT\text{-}H)^-$ product ion. It is generally accepted that this product ion is formed by the direct proton abstraction of neutral TNT by O_2^- reactant ions. Data presented here demonstrate the reaction involves the formation of an intermediate $(TNT{\cdot}O_2)^-$, from the association of either $TNT + O_2^-$ or $TNT^- + O_2$. This intermediate has two subsequent reaction branches. One of these branches involves simple dissociation of the intermediate to TNT^-; the other branch is a terminal reaction that forms the typically observed $(TNT\text{-}H)^-$ ion via proton abstraction. The dissociation reaction involving electron transfer to TNT^- appeared to be kinetically favored and prevailed at low concentrations of oxygen (less than 2%). The presence of significant amounts of oxygen, however, resulted in the predominant formation of the $(TNT\text{-}H)^-$ ion by the terminal reaction branch. With TNT^- in the system, either from direct electron attachment or by simple dissociation of the intermediate, increasing levels of oxygen in the system will continue to reform the intermediate, allowing the cycle to continue until proton abstraction occurs. Key to understanding this complex reaction pathway is that O_2^- was observed to transfer an electron directly to neutral TNT to form the TNT^-. At oxygen levels of less than 2%, the TNT^- ion intensity increased with increasing levels of oxygen (and O_2^-) and was larger than the $(TNT\text{-}H)^-$ ion intensity. As the oxygen level increased from 2 to 10%, the $(TNT\text{-}H)^-$ product ion became predominant. The potential reaction mechanisms were investigated with an ion mobility spectrometer, which was configured to independently evaluate the ionization pathways. (Int J Mass Spectrom 214 (2002) 257–267) Published by Elsevier Science B.V.

1. Introduction

Ion mobility spectrometry (IMS) is an analytical tool based on formation and separation of gas phase ions at atmospheric pressure in a weak electric field [1–3]. In a typical IMS ionization source, ^{63}Ni emits beta particles that interact with the buffer gas (typically nitrogen and oxygen) to produce a source of electrons, which quickly reach low, near thermal, energies at atmospheric pressure [1,2]. When air is used as the instrument gas, these low energy electrons initially react with oxygen, leading to the formation of O_2^- ions. The O_2^- reacts with trace gases and water found in the air to subsequently form negative reactant ions, such as: $(H_2O)_nO_2^-$, $(H_2O)_n(CO_2)_mO_2^-$, and NO^- [4]. The negative reactant ions participate in gas phase reactions with an analyte to form the product ions. The relative importance and direction of these reactions depends on the competitive distribution of the available charge and is based on the gas phase acidity (or basicity), electron affinity, and concentration of the competing species [2].

A common explosive, 2,4,6-trinitrotoluene (TNT) is known to have several ionization pathways that form

* Corresponding author. E-mail: ewinrg@inel.gov

1387-3806/02/$20.00 Published by Elsevier Science B.V.
PII S1387-3806(01)00591-7

negative product ions at reduced pressure in mass spectrometry [5,6]. At the atmospheric pressure conditions present in IMS, however, TNT forms only the $(TNT\text{-}H)^-$ and TNT^- product ions [7–11]. In the routine analysis of explosives by IMS, it has become standard practice to add a chlorinated hydrocarbon to the ionization region to form chloride reactant ions [12,13]. Under these conditions, only the proton abstracted $(TNT\text{-}H)^-$ ion is observed, and it is exclusively used for detection of TNT. The Cl^- reactant ions are used to minimize the effect of electron transfer reactions involving molecular oxygen and trace gases found in air, making both reactant and product ion spectra easier to interpret because of the elimination of extraneous peaks [14,15].

When only air is used as the instrument gas (no Cl^- reactant ions present), $O_2{}^-$ reactant ions are dominant. Under these conditions, the proton abstracted $(TNT\text{-}H)^-$ ion is again the only product ion observed [7,8]. It is generally accepted that $O_2{}^-$ in the ionization region of the IMS instrument acts as a Brønsted base to abstract a proton from TNT to form the $(TNT\text{-}H)^-$ product ion by Eq. (1) [7,8,10].

$$TNT + O_2{}^- \rightarrow (TNT\text{-}H)^- + HO_2 \quad (1)$$

In Eq. (1), the proton abstraction enthalpy for TNT is endothermic ($\Delta H_r^\circ = 315.6$ kcal/mol), while the proton association enthalpy of $O_2{}^-$ is exothermic ($\Delta H_r^\circ = -352.7$ kcal/mol). These thermodynamic values are listed in Table 1. The overall enthalpy for the reaction in Eq. (1) is, therefore, exothermic ($\Delta H_r^\circ = -37.1$ kcal/mol). Exothermic proton transfer reactions generally proceed at the capture rate [16].

Table 1
Thermodynamic values for listed reactions (values are in kcal/mol)

Reaction	ΔH_r°	Reference
$O_2 + e^- \rightarrow O_2{}^-$	−10.4	[17]
$TNT + e^- \rightarrow TNT^-$	−38.9	[18]
$O_2{}^- + H^+ \rightarrow HO_2$	−352.7	[15]
$TNT \rightarrow (TNT\text{-}H)^- + H^+$	315.6	[18]
$TNT + O_2{}^- \rightarrow (TNT\text{-}H)^- + HO_2$	−37.1	Calculated
$TNT + O_2{}^- \rightarrow TNT^- + O_2$	−28.5	Calculated

The TNT^- product ion is formed in the absence of oxygen (nitrogen only) by the direct attachment of the near thermal electrons to the neutral TNT molecule as shown in Eq. (2) [7,8,10].

$$TNT + e^- \rightarrow (TNT^-)^* \overset{N_2}{\rightarrow} TNT^- \quad (2)$$

At atmospheric pressure conditions of IMS, the initially excited $(TNT^-)^*$ ion is stabilized by collisions with the buffer gas molecules.

It is also reasonable to expect that TNT^- can be formed by charge exchange with anions (M^-) when the electron affinity of TNT is greater than that of the neutral molecule, M (Eq. (3)).

$$TNT + M^- \overset{N_2}{\rightarrow} TNT^- + M \quad (3)$$

It is expected that oxygen can act in this role since TNT has a greater electron affinity than oxygen (Table 1). Several studies have noted that even trace levels of molecular oxygen can serve as electron transfer agents in gas phase ion–molecule reactions [17–20]. Since chloride reactant ions are routinely used in the analysis of TNT, $O_2{}^-$ reactant ions and the associated reactions are not observed, because of the high electron affinity of Cl^-. When Cl^- reactant ions are eliminated, these other reactions can be observed.

Although the direct proton abstraction reaction (Eq. (1)) is generally accepted [7,8,10] data here will show that the observed $(TNT\text{-}H)^-$ product ion forms through a more complex mechanism, which involves the formation of the $[TNT{\cdot}O_2]^-$ intermediate. This intermediate can be formed by the either the association of TNT with $O_2{}^-$ or the association of O_2 with TNT^-. From this intermediate, two separate reactions can occur. First is a simple dissociation of the intermediate leaving the charge on TNT, which has the higher electron affinity, forming TNT^-. The second reaction of the intermediate involves the abstraction of a hydrogen atom from TNT, which yields $(TNT\text{-}H)^-$ product ion and HO_2 neutral. Both of these reactions stemming from the same intermediate have not been reported, although Spangler and Lawless [8] have suggested that the formation of the $(M-H)^-$ product

ion for dinitrotoluene might proceed through the electron attached (M^-) product ion.

The experiments presented here investigate the ion–molecule reaction pathways involving oxygen and TNT. Reactions were isolated for investigation by configuring the delivery of oxygen at various concentrations into separate regions of the IMS instrument. The results clearly show the transfer of an electron to TNT from O_2^- and demonstrate hydrogen atom abstraction from TNT^- by neutral O_2.

2. Experimental methods

2.1. Chemicals

TNT (Supelco, Bellefonte, PA) was diluted to 5 ng/μL from 99.9% pure stock standards (1 mg/mL) using 99.8% pure acetone (Aldrich). Ultra high purity nitrogen, was provided by compressed gas bottle (US Welding, Denver, CO). Gas standards of oxygen in nitrogen were purchased from Scott Specialty Gases (Plumsteadville, PA) in specific concentrations of 0.1, 0.5, 1.0, 2.0, 5.0, and 10.0% oxygen in nitrogen with an analytical accuracy of ±5%.

2.2. Instrumentation

Experiments were conducted using a Phemto-Chem Ion Mobility Spectrometer Model 110, as diagrammed in Fig. 1 (PCP, Inc., West Palm Beach, FL). The drift tube was 14 cm long, with an 8 cm drift region (4.25 cm diameter) and a 6 cm ionization region.

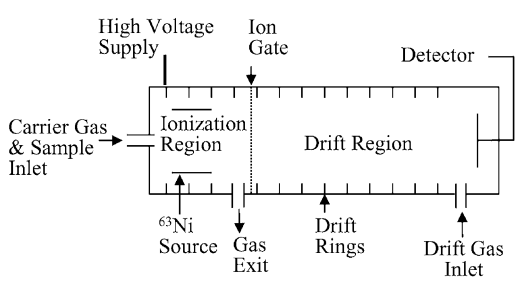

Fig. 1. Diagram of the PCP model 110 IMS instrument.

During most of the experiments, the carrier gas flow rate was kept at 100 mL/min with the drift gas at 500 mL/min. In the injected air experiments, 15 mL of air was added to the drift gas by syringe injection through a gas tight septum during the analysis of TNT. To minimize the presence of oxygen in the ionization region during the injected air experiments, the carrier gas flow was increased to 250 mL/min and the drift flow was reduced to 325 mL/min. Flows were maintained at constant levels using mass flow controllers (Hastings Models 200 and 202, Hampton, VA). The IMS drift field was maintained at 200 V/cm. The IMS instrument was operated at atmospheric pressure which, over the duration of the experiments, varied from 635 to 650 mmHg (as measured with a mercury barometer). Operating temperature was either 100 or 150 °C (as measured by a type K thermocouple).

The gas flows for the PCP IMS instrument used in these studies are shown in Fig. 1. In this design, the carrier gas flow brings reagent gases and sample into the ionization region and the drift gas enters near the detector and flows countercurrent to the carrier gas. There is a common gas exit for both flows that is located near the ion gate, between the ionization region and drift region of the IMS. Most IMS configurations have a unidirectional flow, with the drift gas sweeping neutral molecules out of the ionization end of the IMS instrument [21]. In the unidirectional flow design, both the drift and carrier gases exit through the ionization region. This design precludes the independent evaluation of neutral molecules that are only in the drift region. The PCP design, with countercurrent flows and a gas exit near the boundary between the ionization region and the drift region, allows for separation of the drift and carrier gas flows so that the effects of chemicals in each region can be independently evaluated.

Potential problems with the drift gas entering the ionization region were controlled by adjustments in the flow rates. To verify that this potential problem was controlled, a 0.1 mL injection of trichloromethane headspace (about 100 μg) was added by syringe injection through a gas tight septum into the drift gas during the analysis of TNT when nitrogen was being used for both instrument gases. An elevated baseline,

at drift times shorter than that expected for Cl^- formed in the ionization region, was observed (indicative of drift region reactions). No discrete Cl^- reactant ion peak was observed at the anticipated drift time and there was also no formation of the $(TNT\text{-}H)^-$ product ion. This indicated that no Cl^- was formed in the ionization region.

2.3. Data collection

The ion gate pulse was 150 μs wide at a frequency of 50 Hz. Each scan contains data points which were collected at a frequency of 25 kHz, with a total of 650 points collected. The signal was then processed by digital signal averaging using an advanced signal processing (ASP) board and software (Graseby Ionics, Watford, UK) in an Intel 80386-based computer. Spectra represent data averaged over 32 scans.

2.4. Formation of reactant ions

The ultra high purity nitrogen was used in both the carrier and the drift to provide 0% oxygen conditions. Although this is labeled "0% O_2", the ultra high purity nitrogen does have traces of oxygen present. This will be noted in some spectra. For the experiments where the oxygen concentration was varied, the gas standards of oxygen in nitrogen were used. The IMS was configured to independently deliver the nitrogen or the oxygen gas mixtures into either the carrier or drift to establish the conditions necessary to investigate reaction pathways. Water concentrations in the nitrogen and oxygen were measured at less than 10 ppm by a hygrometer (Panametrics, Moisture Image Series 1, Waltham, MA).

2.5. TNT analysis

TNT was introduced into the IMS by two methods. Individual samples, discussed in Table 2 and Figs. 5 and 7, were prepared by using 1 μL of the 5 ng/μL dilute solution of TNT that was placed onto a standard PCP quartz tube (4.0 mm i.d., 5.5 mm o.d., 40.0 mm long) using a syringe (Hamilton No. 701, Reno, NV). The acetone solvent was then allowed to evaporate for 30 s prior to placing the quartz tube directly into the inlet of the IMS. The heated carrier gas stream then flowed through the quartz tube, where the analyte was thermally desorbed and swept into the IMS ionization region.

The analyses discussed in Figs. 2 and 8 were accomplished by adding headspace vapor desorbed from TNT coated glass beads into the IMS carrier gas. After introduction, a reliable TNT signal was produced in the IMS for about 10 min before additional TNT was added. The low energy electron peak in the spectrum was reduced significantly. From the peak intensity, the TNT concentration in the carrier gas was estimated to be about 250 pg/mL. The intent was not to control the concentration of TNT, but rather to maintain the TNT concentration at a reasonably high level for several minutes so that data could be collected for the injected air experiments.

A final experiment was designed to convert nearly all of the free electrons in the ionization region to TNT^-. This was accomplished by adding significant quantities of TNT to the ionization region until the electron peak was nearly depleted. As with the data for Figs. 2 and 8, TNT vapor was desorbed from TNT coated glass beads and added to the IMS carrier gas while monitoring the electron peak intensity. Nitrogen was used in both the carrier gas and the drift gas. Injections of pure oxygen (2, 3, 5 and 10 mL) were added through a septum in the drift gas line.

3. Results and discussion

Central to the investigation of reaction mechanisms using IMS is the concept that reactions take place in both the ionization region and the drift region of the instrument. By isolating a reactant to either region, the corresponding reaction can be monitored. Although drift region reactions degrade resolution during routine analysis [2], they are useful in the study of ion–molecule reactions. A spectrum showing both of these types of reactions for the analysis of TNT is shown in Fig. 2. This spectrum was collected when

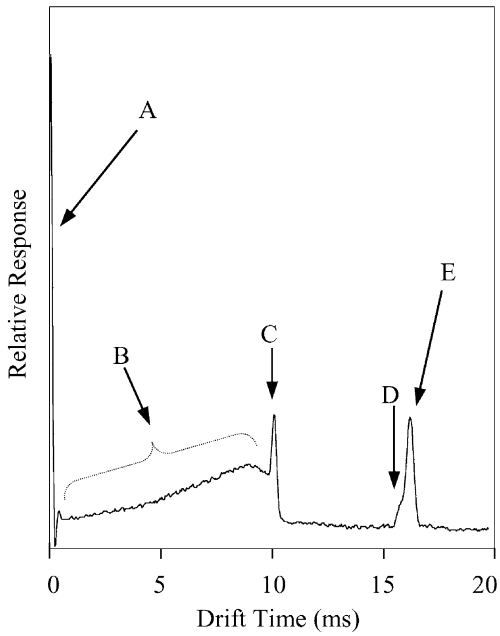

Fig. 2. Spectrum of TNT analysis in N_2 in the carrier gas and air the drift gas at 100 °C. (A) Near thermal electrons, (B) O_2^- ions formed in the drift region, (C) O_2^- ions formed in the ionization region, (D) indicates the location of $(TNT\text{-}H)^-$ ions formed in the ionization region, and (E) TNT^- ions formed in the ionization region. $(TNT\text{-}H)^-$ ions are being formed in the drift region and therefore, appear as a leading shoulder on the left of the TNT^- peak between points D and E.

nitrogen was used as the carrier gas and air (∼20% O_2) was used as the drift gas. For this spectrum, the IMS was operated at 100 °C. Point (A) in Fig. 2 corresponds to the drift time of low energy electrons, while point (C) is the drift time of O_2^- ions formed in the ionization region and introduced into the drift tube through the ion gate. The elevated baseline indicated by area (B) comes from reactions of oxygen with low energy electrons taking place in the drift region, while separation is occurring. Because this reaction takes place between the ion gate and the detector, there is a distribution of drift times that fall between that of low energy electrons and O_2^- formed in the ionization region. The distribution relates to the locations in the drift region where the reactions take place. Point (E) is the drift time of TNT^- ions, while point (D) is the expected drift time of $(TNT\text{-}H)^-$ ions formed in the ionization region, based on the mobility values reported by other researchers [7–11]. Since this spectrum was collected at 100 °C, the drift times of both of the TNT ions will be somewhat slower than in the subsequent spectra collected at 150 °C. The $(TNT\text{-}H)^-$ in this spectrum is being formed by a reaction occurring in the drift region and therefore appears as a leading shoulder (elevated baseline) on the TNT^- peak. An elevated baseline between expected peak positions is an indication that reactions are occurring in the drift region. Information from these drift region reactions can be used to investigate ionization mechanisms.

Ion formation in IMS depends mostly on the competitive distribution of the available charge, thus, the gas phase enthalpies of reaction (Table 1) of the competing species are important in the evaluation of the ionization mechanism of TNT. These values have been used to evaluate reactions for which no thermodynamic data exist and to construct an energy level diagram of the potential reactions in the ionization of TNT (Fig. 3). The generally accepted direct proton abstraction reaction of TNT by O_2^- is known to be exothermic ($\Delta H_r^\circ = -37.1$ kcal/mol) (Table 1). An alternative mechanism investigated here is also thermodynamically feasible. The initial step of the

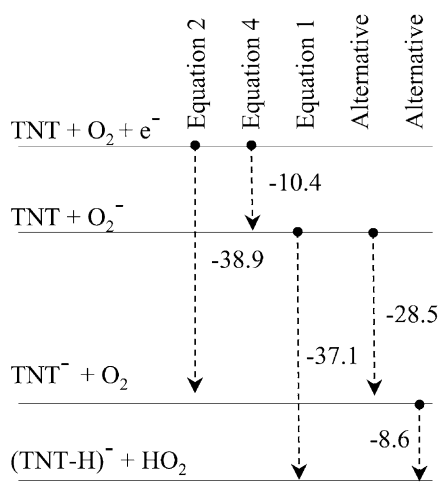

Fig. 3. Energy diagram for the reactions of TNT, O_2 and e^-. Units are in kcal/mol. These energy differences are referenced in Table 1 or are calculated differences from values in Table 1.

transfer of an electron from O_2^- to TNT is exothermic ($\Delta H_r^\circ = -28.5$ kcal/mol) and the subsequent abstraction of a hydrogen atom from TNT^- by neutral O_2 is also exothermic ($\Delta H_r^\circ = -8.6$ kcal/mol). Although the second reaction of this alternative mechanism is slightly exothermic, it is not observed to be as efficient as the electron transfer from O_2^- to TNT. However, at the high oxygen concentrations found in air (~20%), there is an abundance of collisions with oxygen which leads to $(TNT\text{-}H)^-$ being the only observed product ion peak in the spectrum.

As oxygen is added to the nitrogen carrier gas of an IMS, O_2^- reactant ions are formed at the expense of the near low energy electrons (Eq. (4)).

$$O_2 + e^- \rightarrow (O_2^-)^* \xrightarrow{N_2} O_2^- \quad (4)$$

The peak area of both the near thermal electrons and the O_2^- reactant ions are shown in Fig. 4 at several oxygen concentrations in both the carrier and drift gases of an IMS instrument. As the amount of added oxygen increases, the low energy electrons decrease and the O_2^- reactant ions increase, clearly showing the relationship between low energy electrons and the O_2^- reactant ions.

Previous studies have found that when nitrogen is used as the IMS instrument carrier gas and near thermal electrons dominate, TNT forms only the electron attachment TNT^- ion by Eq. (2) [7,8,10,11]. When air (~20% O_2) is used as the carrier gas, and O_2^- reactant ions are present, only $(TNT\text{-}H)^-$ product ions are observed [7,8,10,11,22] When increasing amounts of oxygen (from about 0.4 to about 4.2%) were added to nitrogen in both the carrier and drift gas regions, a continuous shift from the TNT^- ion to the $(TNT\text{-}H)^-$ ion occurs [8]. The data collected here and presented in Fig. 5 confirm this shift from the TNT^- ion to the $(TNT\text{-}H)^-$ ion. The ionization yield for $(TNT\text{-}H)^-$ at higher oxygen concentrations is also substantially greater than the ionization yield for TNT^- in nitrogen. This is apparent in Fig. 5, and has been noted by Karasek and Denney [7].

Of specific importance for the evaluation of the alternative mechanism are the data in Fig. 5 that show the amount of TNT^- ion increases as the amount of added oxygen increases to 1.0% and then decreases at higher concentrations. These data indicate that O_2^- directly transfers an electron to TNT to form the TNT^- ion. The presence of this reaction establishes a basis that the formation of the $(TNT\text{-}H)^-$ ion can take place by abstraction of a hydrogen atom from the TNT^- ion by neutral O_2.

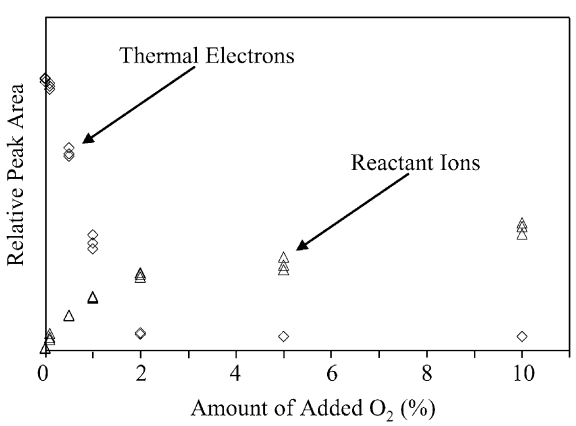

Fig. 4. A plot of peak area at several O_2 concentrations in N_2 buffer gas (in both the carrier and drift gas) for thermal electrons and reactant ions (O_2^-). Three measurements were taken at each O_2 concentration.

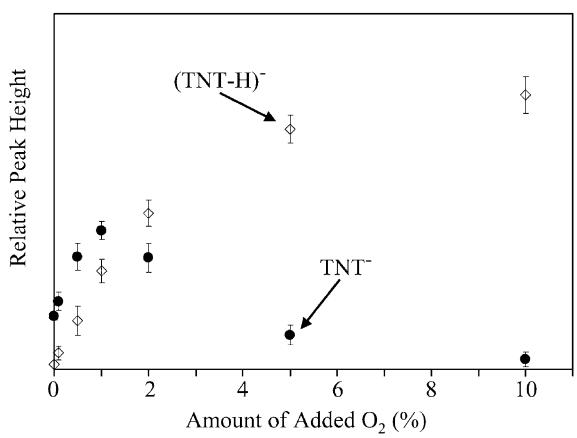

Fig. 5. A plot of peak height at several O_2 concentrations in N_2 buffer gas (in both the carrier and drift gas) for $(TNT\text{-}H)^-$ and TNT^- product ions. Three measurements were taken at each O_2 concentration with the averages plotted.

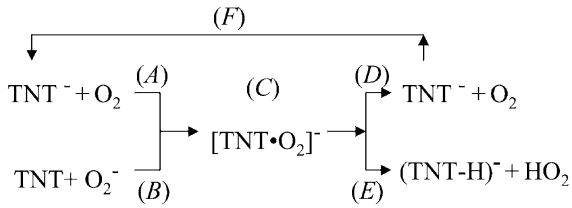

Fig. 6. Diagram of possible anion/neutral reactions between TNT and O_2.

The possible reaction pathways are represented in Fig. 6. The direct abstraction of a proton from TNT by O_2^- is the pathway {B, C, E}, the hydrogen atom abstraction of TNT^- by neutral O_2 is the pathway {A, C, E}, electron transfer from O_2^- to TNT is {B, C, D}, and a non-productive equilibrium is established through {A, C, D}. All reaction mechanisms proceed through a common intermediate $[TNT{\cdot}O_2]^-$, which is marked as {C}. Once $[TNT{\cdot}O_2]^-$is formed, the reaction can proceed to the proton abstraction of TNT {C, E} or dissociation to O_2 and TNT^- {C, D}. When TNT^- is formed {C, D}, it can combine with the additional neutral O_2 present {F} and lead to the reformation of $[TNT{\cdot}O_2]^-$ through {A, C}. Although not listed in Fig. 6, TNT^- ions can also be formed through direct attachment of a low energy electron to TNT. The thermodynamic endpoint of these reactions is the formation of $(TNT\text{-}H)^-$ ion {E}.

In atmospheric pressure conditions, electron capture or transfer reactions can occur at nearly every collision [23]. Because of their difference in electron affinity, the transfer of the electron from O_2^- directly to TNT is expected. Since the formation of O_2^- reactant ions approaches saturation at levels near 2% oxygen added to the carrier gas (Fig. 4), further addition of oxygen mainly adds more neutral O_2 to the system. The dramatic decline in TNT^- and increase in $(TNT\text{-}H)^-$ shown in Fig. 5, at oxygen concentrations greater than 2%, can therefore, be attributed to the presence of neutral O_2, which abstracts a hydrogen atom from TNT^- through reaction {A, C, E} in Fig. 6.

Reaction {A, C, E} can be isolated from the other potential reactions by control and separation of the drift and carrier gas flows within the PCP IMS instrument. The PCP design, with the placement of the gas exit near the ion gate and the countercurrent flow of gases (Fig. 1), allows this control and the independent study of effects of chemicals in each flow. For the initial investigation of pathway {A, C, E}, the IMS instrument was set up in two configurations. In the first configuration, various oxygen gas mixtures were used as the carrier gas while only nitrogen was used as the drift gas. Both TNT product ions would only be formed in the ionization region. In this configuration, the presence of only nitrogen in the drift gas eliminated the possibility of drift region reactions involving oxygen. The second configuration had the same oxygen gas mixtures used as both the carrier and the drift gas. This configuration allowed the oxygen in the drift region to influence the reaction. The analysis of TNT in each of these configurations allowed the comparison of the relative quantity of the two product ions formed with various amounts of neutral O_2 added to the carrier gas in one configuration and to both the carrier and drift gases in the other configuration.

The data from the analysis of TNT in the two gas flow configurations are presented in Table 2. The ratio of the $(TNT\text{-}H)^-$ to the TNT^- ions was determined in each configuration for each oxygen concentration. Data reported in Table 2 are averages of triplicate analyses. With only nitrogen present, the TNT^- ion dominates. If nitrogen is kept in the drift region with increasing oxygen in the carrier gas, the ratio of $(TNT\text{-}H)^-$ to TNT^- steadily increases to almost 6 at

Table 2
Peak area ratios of the $(TNT\text{-}H)^-$ to the TNT^- product ions with varying amounts of oxygen in the carrier gas, with and without oxygen in the drift gas

Percent O_2 in the carrier gas	$(TNT\text{-}H)^-/TNT^-$	
	N_2 in drift gas	Same concentration of O_2 in drift gas as in carrier gas
0.0 (N_2 only)	0.11	0.11
0.1	0.15	0.24
0.5	0.19	0.45
1.0	0.26	0.71
2.0	0.93	1.41
5.0	2.34	7.41
10.0	5.98	36.24

10.0% O_2. All of the $(TNT\text{-}H)^-$ was formed in the ionization region under these conditions.

Substantially different results are found when oxygen is introduced into both the carrier and drift gases. At each oxygen concentration, the ratio of $(TNT\text{-}H)^-$ to TNT^- increases, reaching a maximum of about 36 at 10.0% O_2. This is six times higher than when nitrogen was used as the drift gas. The increase in the ratio must come from the conversion of TNT^- to $(TNT\text{-}H)^-$ through the influence of neutral O_2 in the drift region, as shown in pathway {A, C, E} of Fig. 6. The procedure for verifying that drift gas did not enter the ionization region was described in the instrumentation section of this paper.

Spectra from four IMS instrument configurations, acquired at 150 °C, are shown in Fig. 7. Spectrum I was collected with nitrogen in both the carrier and drift and shows only the TNT^- peak. Spectrum II was collected when 5.0% O_2 was added to the nitrogen carrier gas while keeping nitrogen drift gas. In this configuration, there are distinct, separate $(TNT\text{-}H)^-$ and TNT^- peaks. Spectrum III was collected with 5.0% O_2 in both the drift and carrier gas. The $(TNT\text{-}H)^-$ ion is dominant, with a hint of TNT^- present (tailing shoulder). Spectrum IV was collected with nitrogen carrier gas and 5.0% O_2 in the drift gas. In this configuration, only TNT^- is formed in the ionization region, while reactions with neutral O_2 take place in the drift region. In Spectrum IV, the peak from TNT^- broadens into the peak position for the $(TNT\text{-}H)^-$ ion, indicating that the $(TNT\text{-}H)^-$ is forming in the drift region from the hydrogen atom abstraction of TNT^- by neutral O_2. Drift region reactions are also noticeable in spectrum III, which has a slight shift of the peak maximum and a tailing shoulder on the $(TNT\text{-}H)^-$ peak. The results of drift region reactions can also be seen in comparing spectrum II and III, where the only difference is addition of oxygen to the drift region.

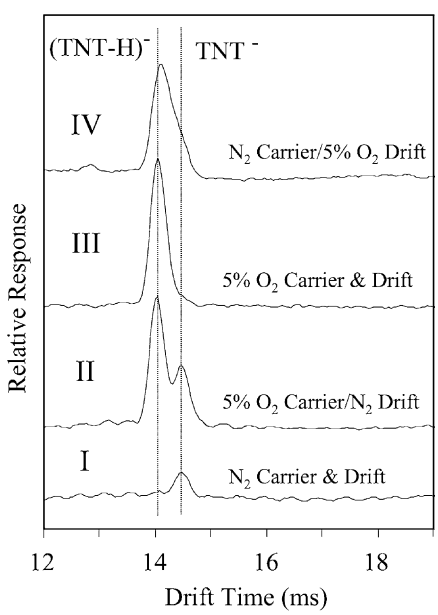

Fig. 7. Spectra from the analysis of TNT with four different gas configurations. Dotted lines indicate the location for the $(TNT\text{-}H)^-$ and TNT^- product ions when formed in the source.

Additional evidence for the production of $(TNT\text{-}H)^-$ from TNT^- in the drift region involved the use of a injection of oxygen into the nitrogen drift gas. In these experiments, nitrogen was used for both the carrier and drift gas. A 15 mL injection of clean air was added to the drift gas by syringe injection through a gas tight septum during the analysis of TNT. The data from spectra collected during the injection are shown in Fig. 8. In the top part of Fig. 8 are two spectra that illustrate the air injection. The upper spectrum was collected immediately after making the injection into the drift region. Line (A) indicates the position of low energy electrons. The elevated baseline (B) is caused as the air injection passes through the drift region and the oxygen reacts with low energy electrons, forming O_2^- ions in the drift region during separation, yielding a distribution of drift times. The TNT^- peak (D) decreases as a small leading shoulder (C) is formed. In the lower spectrum, the injection of air is approaching the gas exit and the elevated baseline is broader and shifted to longer drift times, indicating that the reactions are occurring closer to the ion gate. There is now a pronounced leading shoulder at (C) indicating the formation of $(TNT\text{-}H)^-$ ions closer to the ion gate in the drift region. The lack of a distinct O_2^- reactant ion peak near 8 ms indicates that no oxygen has reached the ionization region where it could form O_2^- ions and abstract a proton from TNT.

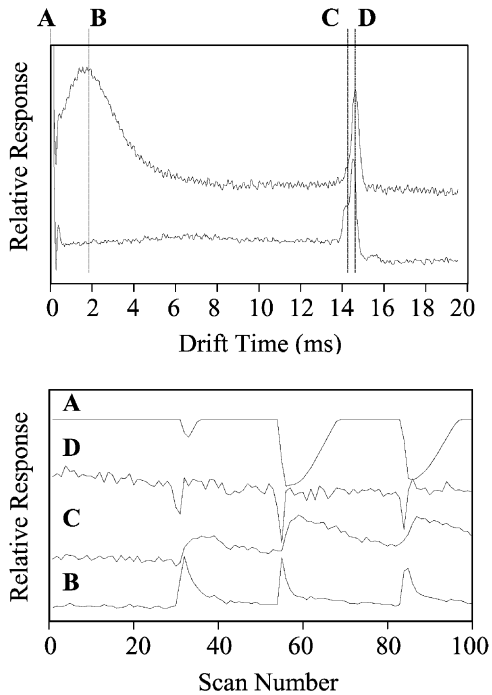

Fig. 8. Spectra and compiled data from the analysis of TNT in N_2 when three injections of air were made into the drift region. The top spectrum was collected immediately after the injection of air while the bottom spectrum was collected a few seconds later after the air moved up the drift region. The bottom half plots are of the intensity at each marker (A–D) in the spectrum with scan number. Each scan represents approximately 1 s. Air injections were made at approximately scan 30, 55 and 85.

In the bottom part of Fig. 8 are the results from 100 spectra or scans collected at about one second intervals during the addition of three injections of air. The spectra were evaluated by monitoring a point on the spectrum corresponding to low energy electrons (A), O_2^- elevated baseline (B), $(TNT\text{-}H)^-$ ions (C), and TNT^- ions (D). The ion current in each window for each scan is plotted verses the scan number. When a injection is made, there is initially a dip in the TNT^- ion (D) as the injection passes through the drift region and neutral O_2 is abstracting a hydrogen atom from TNT^-. The dip in low energy electrons (A) and increases in $(TNT\text{-}H)^-$ ion (C) and O_2^- elevated base line (B) lag the dip in TNT^- as the injection of air moves through the drift region. The estimated linear velocity of the injected air through the drift region is about 20 cm/min. The pattern is the same for all three injections. When only nitrogen is present, only the TNT^- ion is observed. As the injection passes through the drift, the neutral O_2 molecules in the drift region abstract a hydrogen atom the TNT^- produced in the ionization region. No O_2^- produced in the ionization region was ever observed in the spectra.

An additional experiment to confirm the production of $(TNT\text{-}H)^-$ from TNT^- with neutral oxygen in the drift region was performed. The experiment was designed to minimize the potential of forming O_2^- in the drift region and thus exclude the possibility of forming $(TNT\text{-}H)^-$ from TNT and O_2^-. As with the previous experiments, pure nitrogen was used in both the drift and carrier gases. In this experiment, however, sufficient TNT was then added to the carrier gas to substantially deplete the low energy electrons that might

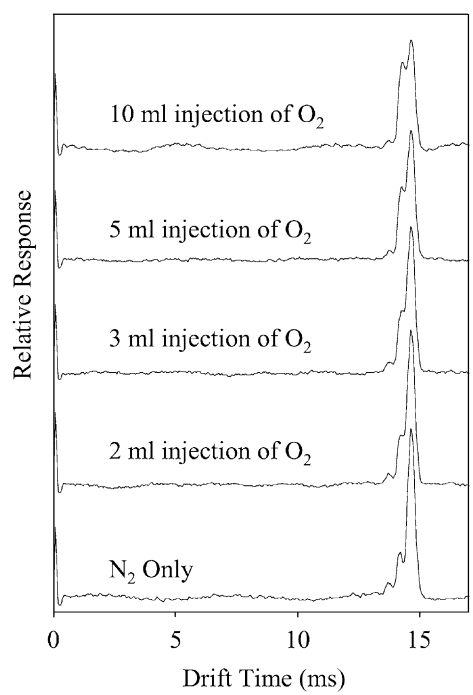

Fig. 9. IMS spectra for TNT at various amounts of pure oxygen added to the nitrogen drift gas. Significant amounts of TNT were added to the source region to significantly reduce the near thermal electrons minimizing the potential of forming O_2^- in the drift region or the ionization region.

promote formation of O_2^- in the drift region and produce a large quantity of TNT^- ions. Successively larger injections of pure oxygen (2, 3, 5, and 10 mL) were then added to the nitrogen drift gas (Fig. 9). The use of pure oxygen allowed for smaller injection volumes while maintaining relatively high oxygen concentrations in the drift region. This minimized both perturbations to the flow system as well as possible adverse effects due to dilution of the TNT sample with increased flow. The results of this experiment are consistent with the previous results. As the size of the oxygen injection increased, the size of the leading shoulder on the TNT^- peak increased, indicating the formation of $(TNT\text{-}H)^-$. This provided additional confirmation that the formation of $(TNT\text{-}H)^-$ from TNT^- was occurring in the drift region under the influence of neutral O_2.

4. Conclusions

The mechanism for the formation of the $(TNT\text{-}H)^-$ product ion in air has been demonstrated to be more complex than direct proton abstraction. With oxygen concentrations increasing from 0 to about 1% in the carrier gas, the amount of TNT^- ions increases. These data indicate the initial ionization step involves the formation of an intermediate, $(TNT{\cdot}O_2)^-$, which rapidly dissociates to TNT^- and O_2 via electron transfer. At higher oxygen concentrations, the amount of TNT^- ion decreased due to the presence of neutral O_2, and reached negligible levels at 10% oxygen. During this change, the $(TNT\text{-}H)^-$ also increased. With additional levels of oxygen in the system, the TNT^- will reform the intermediate. Another reaction pathway for this intermediate involves proton abstraction from TNT yielding $(TNT\text{-}H)^-$ and HO_2. The $(TNT\text{-}H)^-$ ion is the thermodynamic endpoint for this reaction and with increases in the oxygen concentration, this ion dominates. This mechanism was investigated by the addition of oxygen to the drift region and TNT to the source region in an attempt to isolate reactions, specifically allowing TNT^- to interact with neutral oxygen. When oxygen was added to the drift region while nitrogen was in the carrier gas $(TNT\text{-}H)^-$ formed as a leading shoulder on the TNT^- ion peak indicating the formation of $(TNT\text{-}H)^-$ in the drift region. These results indicate that the predominant product ion formed for TNT in air at atmospheric pressure is the proton abstracted anion. However, the ionization involves the initial transfer of an electron from O_2^- to TNT and the subsequent abstraction of a hydrogen atom from TNT^- by neutral O_2. The proton abstraction step occurs after repeated formation of the $(TNT{\cdot}O_2)^-$ intermediate.

Although the $(TNT\text{-}H)^-$ product ion is used for identification in the routine analysis of TNT, the TNT^- product ion is also characteristic for TNT and may be used for identification [7,10,24]. Since IMS is sometimes susceptible to masking or misidentification of analytes due to peak overlap with interfering compounds, manipulation of the ion chemistry to promote both the $(TNT\text{-}H)^-$ and TNT^- product ions would increase the reliability of identification of TNT in the presence of interfering compounds. The maximum TNT^- peak was found near 1.0% oxygen and may be used to verify the presence of TNT.

Acknowledgements

The authors would like to thank W. Berk Knighton of Montana State University for his helpful discussions of the topics leading to this research. This work was supported through the INEEL Long-Term Research Initiative Program under DOE Idaho Operations Office Contract DE-AC07-99ID13727.

References

[1] H.H. Hill Jr., W.F. Siems, R.H. St. Louis, D.G. McMinn, Anal. Chem. 62 (1990) 1201A–1209A.
[2] G.A. Eiceman, Z. Karpas, Ion Mobility Spectrometry, 1st Edition, CRC Press, Boca Raton, 1994, p. 221.
[3] M.J. Cohen, Time of Flight Ion Analysis with a Pulsed Ion Source Employing Ion-Molecule Reactions, US Patent 3,593,018 (1971) Franklin GNO Corporation, West Palm Beach, FL, USA.
[4] G.E. Spangler, C.I. Collins, Anal. Chem. 47 (1975) 393–402.

[5] J. Yinon, D. Faisse, I.J. Dagley, Org. Mass Spectrom. 26 (1991) 867–874.
[6] M.L. Langford, J.F.J. Todd, Org. Mass Spectrom. 28 (1993) 773–779.
[7] F.W. Karasek, D.W. Denney, J. Chromatogr. 93 (1974) 141–147.
[8] G.E. Spangler, P.A. Lawless, Anal. Chem. 50 (1978) 884–892.
[9] G.E. Spangler, J.P. Carrico, D.N. Campbell, J. Testing Eval. 13 (1985) 234–240.
[10] S.D. Huang, L. Kolaitis, D.M. Lubman, Appl. Spectrosc. 41 (1987) 1371–1376.
[11] G.R. Asbury, J. Klasmeir, H.H. Hill Jr., Talanta 50 (2000) 1291–1298.
[12] V. Lopez-Avila, H.H. Hill Jr., Anal. Chem. 69 (1997) 289R–305R.
[13] R.G. Ewing, D.A. Atkinson, G.A. Eiceman, G.J. Ewing, Talanta 54 (2001) 515–529.
[14] C.J. Proctor, J.F.J. Todd, Anal. Chem. 56 (1984) 1794–1797.
[15] A.H. Lawrence, P. Neudorfl, Anal. Chem. 60 (1988) 104–109.
[16] A.G. Harrison, Chemical Ionization Mass Spectrometry, 2nd Edition, CRC Press, Boca Raton, 1992, p. 208.
[17] I. Dzidic, D.I. Carroll, R.N. Stillwell, E.C. Horning, J. Am. Chem. Soc. 96 (1974) 5258–5259.
[18] I. Dzidic, D.I. Carroll, R.N. Stillwell, E.C. Horning, Anal. Chem. 47 (1975) 1308–1312.
[19] W.B. Knighton, J.A. Bognar, E.P. Grimsrud, J. Mass Spectrom. 30 (1995) 557–562.
[20] W.B. Knighton, T.M. Miller, A.A. Viggiano, R.A. Morris, J.M. Van Doren, J. Chem. Phys. 109 (1998) 9632–9633.
[21] M.A. Baim, H.H. Hill Jr., Anal. Chem. 54 (1982) 38–43.
[22] K.A. Daum, D.A. Atkinson, R.G. Ewing, W.B. Knighton, E.P. Grimsrud, Talanta 54 (2001) 299–306.
[23] L.G. Christophorou, D.L. McCorkle, A.A. Christodoulides, Electron attachment processes, in: L.G. Christphorou (Ed.), Electron–Molecule Interactions and Their Applications, Academic Press, New York, 1984.
[24] G.E. Spangler, Principles underlying the performance of ionization detectors for explosive vapor detection, in: Proceedings of the New Concept Symposium and Workshop on Detection and Identification of Explosives, 1978, Reston, VA.